



## Research Paper

## Development of a control algorithm aiming at cost-effective operation of a VRF heating system



Jin Woo Moon<sup>a</sup>, Young Kwon Yang<sup>a</sup>, Eun Ji Choi<sup>a</sup>, Young Jae Choi<sup>a</sup>, Kwang-Ho Lee<sup>b</sup>,  
Yong-Shik Kim<sup>c</sup>, Bo Rang Park<sup>a,\*</sup>

<sup>a</sup> School of Architecture and Building Science, Chung-Ang University, Seoul, South Korea

<sup>b</sup> Department of Architectural Engineering, Hanbat National University, Daejeon, South Korea

<sup>c</sup> Department of Architectural Engineering, Incheon National University, Incheon, South Korea

## HIGHLIGHTS

- Cost-effective algorithm was developed for the control of VRF heating system.
- ANN model was embedded in the algorithm to determine the cost-effective operation.
- ANN stably predicted the cost for space heating.
- Proposed algorithm saved the heating cost compared to the conventional method.

## ARTICLE INFO

## Keywords:

Variable refrigerant flow heating system  
Artificial neural network  
Predictive controls  
Energy cost

## ABSTRACT

This study aims to develop a control algorithm that can operate an intermittently working variable refrigerant flow (VRF) heating system in a cost-effective manner. An artificial neural network (ANN) model, which is designed to predict the heating energy cost during the next control cycle, is embedded in the control algorithm. By comparing the predicted energy costs for the different setpoint combinations for the system parameters, such as the air handling unit (AHU) supply air temperature, condensing warm fluid temperature, condensing warm fluid amount, and refrigerant condensing temperature, the control algorithm can determine the most cost-effective setpoints to optimally operate the heating system. Two major processes are conducted—development of the predictive control algorithm in which the ANN model is embedded, and performance tests in terms of prediction accuracy and cost efficiency using computer simulation. Results analysis reveals that the ANN model accurately predicts the energy cost, presenting a low coefficient of variation of the root mean square error value (7.42%) between the simulated and predicted results. In addition, the predictive control algorithm significantly saves on the heating energy cost by as much as 7.93% compared with the conventional heuristic control method. From the results analysis, the ANN model and the control algorithm show the potential for prediction accuracy and cost-effectiveness of the intermittently working VRF heating system.

## 1. Introduction

A key objective in the design of enclosed spaces is the provision of a comfortable indoor environmental quality (IEQ). When an appropriate IEQ is provided, occupants feel comfortable, healthy, and safe, with increased attentiveness and productivity [1]. Thermal comfort (TC) is one of the important factors that determine the IEQ. To provide appropriate TC, a thermal conditioning process using equipment such as heating and cooling systems needs to be properly employed.

Sophisticated thermal control systems and strategies can support a comfortable and energy-efficient system operation. A variable refrigerant flow (VRF) system, which is an advanced type of centralized system, has been increasingly applied to condition the indoor thermal environment in recent mid- to high-rise buildings. A VRF system is designed to properly control buildings that have a wide load variation, such as office rooms, commercial buildings, and hotels. Since the refrigerant flow rate to multiple indoor units is determined by electronic expansion valves, each zone can operate individually by a partial

\* Corresponding author.

E-mail addresses: [gilerbert73@cau.ac.kr](mailto:gilerbert73@cau.ac.kr) (J.W. Moon), [dora84@naver.com](mailto:dora84@naver.com) (Y.K. Yang), [ejchl77@gmail.com](mailto:ejchl77@gmail.com) (E.J. Choi), [chlyoungwo@gmail.com](mailto:chlyoungwo@gmail.com) (Y.J. Choi), [kwhl33@hanbat.ac.kr](mailto:kwhl33@hanbat.ac.kr) (K.-H. Lee), [newkim@inc.ac.kr](mailto:newkim@inc.ac.kr) (Y.-S. Kim), [pbr\\_1123@naver.com](mailto:pbr_1123@naver.com) (B.R. Park).

<https://doi.org/10.1016/j.applthermaleng.2018.12.044>

Received 25 August 2018; Received in revised form 6 December 2018; Accepted 8 December 2018

Available online 10 December 2018

1359-4311/ © 2018 Elsevier Ltd. All rights reserved.

**Nomenclature**

BGR	boiler gas consumption rate, kWh
CAPFT	heating capacity ratio according to the entering warm fluid and inlet wet-bulb air temperatures, dimensionless
DX AHU	direct expansion air handling unit
CMH	flow rate of warm fluid
$COP_{REF}$	reference coefficient of performance, 4.787 W/W
$COST_{TOT}$	total energy cost for heating, Korean Won
EA	exhausted air
EIRFLPM	electric input ratio according to the flowrate of warm fluid, dimensionless
EIRFPLR	electric input ratio according to the part load ratio, dimensionless
EIRFRC	electric input ratio according to the refrigerant condensing temperature, dimensionless
EIRFT	electric input ratio according to the entering warm fluid and inlet wet-bulb air temperatures, dimensionless
$\epsilon_{tot}$	fan total efficiency, dimensionless
FF	flow fraction
m	current air mass flow, kg/s
$f_{pl}$	fraction of full load power, dimensionless
gwlpm	amount of warm fluid, L/min
$LOAD_{HEAT}$	average heating load for last control cycle, kW
LR	learning rate
m	air flow, kg/s
$m_{design}$	design (maximum) air flow, kg/s
MO	momentum
NHL	number of hidden layers
NHN	number of hidden neurons
NIN	number of input neurons

NON	number of output neurons
OA	outdoor air
$Q_{OUTUNT}$	reference capacity of the outdoor unit, kW
$Q_{tot}$	fan power, W
OUER	sum of evaporation heat loss of outdoor units, kWh
$P_{CT}$	electric power of the pumps, kW
PLR	part load ratio, %
$P_{OUTUNT}$	electric power of the outdoor unit, kW
RA	returned air
RC	refrigerant condensing temperature, °C
SA	supply air
$t_{CF}$	average condenser fluid temperature for last control cycle, °C
$t_{CF\_SET}$	setpoint of condensing warm fluid temperature, °C
$t_{CUR\_IA}$	current indoor air temperature, °C
$t_{IA}$	average indoor air temperature of zones for last control cycle, °C
$t_{OA}$	average outdoor air temperature for last control cycle, °C
$t_{RF\_SET}$	setpoint of refrigerant condensing temperature, °C
$t_{SA}$	average supply air temperature of AHUs for last control cycle, °C
$t_{SA\_SET}$	setpoint of air handling unit supply air temperature, °C
$t_{SETPOINT}$	indoor setpoint temperature for the heating system, °C
$V_{CF}$	average condensing warm fluid amount for control cycle, L/min
$V_{CF\_SET}$	setpoint of condensing warm fluid amount, L/min
X	inlet air wet-bulb temperature entering the DX coil in the AHU, °C
Y	entering warm fluid temperature
$\rho_{air}$	air density at standard conditions, kg/m <sup>3</sup>
$\Delta P$	fan design pressure increase, Pa

heating load. Actively responding to the load variation, the VRF system is able to control the system more energy-efficiently, proving a comfortable indoor thermal environment [2]. Section 2 provides detailed information regarding the VRF system.

Despite the advantages, there is a principal issue to be addressed for more appropriate control of the VRF system. The setpoints of the VRF

system parameters have been determined in a heuristic manner. The setpoints of the air handling unit (AHU) supply air temperature ( $t_{SA\_SET}$ ), the condensing warm fluid temperature ( $t_{CF\_SET}$ ), the condensing warm fluid amount ( $V_{CF\_SET}$ ), and the refrigerant condensing temperature ( $t_{RF\_SET}$ ) are generally set as constant values without cost-effective consciousness. Under this circumstance, the opportunity for

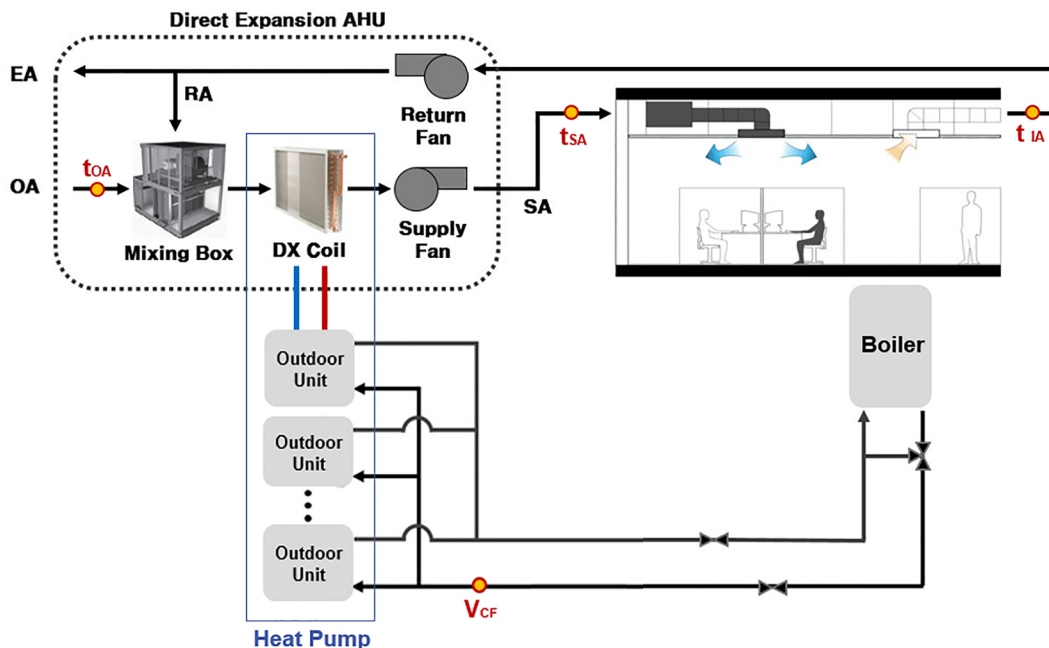


Fig. 1. Diagram of the direct expansion (DX) air handling unit (AHU)-water source VRF.

more cost-effective space thermal conditioning in the current control method is missing.

This study aims at developing a predictive control algorithm that can operate the VRF heating system based on the consideration of cost-effectiveness. An artificial neural network (ANN) model, which predicts the heating energy cost during the next control cycle for the different setpoints of the control variables was developed and embedded in the control algorithm. Using the predicted energy cost for different setpoint combinations, the control algorithm can determine the variables' optimal setpoints for operating the heating system.

Two major processes are conducted to propose the cost-effective predictive heating system control method. The first process is to develop a predictive control algorithm in which the ANN model is embedded, and the second process is to test its performance in comparison with the conventional heuristic control method, which uses fixed values for the control variables (e.g., 38 °C for the supply air temperature). The potential of the optimally determined operating strategy is presented through a results analysis.

## 2. Review of the VRF heating system and the ANN

### 2.1. VRF heating system

Fig. 1 shows the direct expansion (DX) AHU water source VRF, which is composed of an AHU, outdoor units, a boiler, and pumps. In the system, the heat source of the VRF system is the hot water produced from the boiler during the heating mode. This means that the boiler provides hot water to the outdoor unit, i.e., evaporator in the heating mode, as the heat source. The outdoor unit (evaporator) and DX coil (condenser) is connected with the refrigerant pipe, through which the refrigerant circulates for the phase change between liquid and gas. Therefore, the heat pump (VRF) pumps heat from the outdoor unit (evaporator) to DX coil (condenser), not from boiler to DX coil. The difference from the conventional AHU system is that hot water is not used in the AHU heating coil, but refrigerant is directly provided to heat

the conditioned air.

Table 1 summarizes recent studies about the VRF system and application. In these studies, the VRF system presents the potential to control the indoor thermal environment more energy-efficiently, supporting a comfortable indoor thermal environment. The VRF heating system can improve energy efficiency because it can properly respond to a wide load variation. Each zone in a building controls the amount of heat supply more dynamically by individual operation of an electronic expansion valve in the indoor unit.

The settings of the system variables are related to the outdoor units, the boiler, the pumps for circulating condenser fluids, and the fans in the AHU. Eqs. (1)–(4) present the electricity and gas consumption by the outdoor units [9–11], boiler, pumps [9,12], and fans in the AHU [9,13,14], respectively. The coefficients in Eqs. (1-1)–(1-5) are derived from both data obtained from field measurements and a technical data book [11]. Similarly, the coefficients in Eqs. (3) and (4-1) are derived from field measurement data from the test building described in Section 5. Thus, these coefficients can only be applied to the particular system installed in the test building.

$$P_{OUTUNT}(\text{kWh}) = Q_{OUTUNT} \times 1/\text{COP}_{REF} \times \text{CAPFT} \times \text{EIRFT} \times \text{EIRFPLR} \times \text{EIRFLPM} \times \text{EIRFRC} \quad (1)$$

$$\text{CAPFT}(\text{dimensionless}) = 1.4926264835 - 0.01393254X - 0.0001548X^2 \quad (1-1)$$

$$\begin{aligned} \text{EIRFT}(\text{dimensionless}) &= 0.8002364 + 0.0179363X + 0.0009182X^2 \\ &\quad - 0.01341544Y + 0.00108534Y^2 - 0.0022828XY \end{aligned} \quad (1-2)$$

$$\begin{aligned} \text{EIRFPLR}(\text{dimensionless}) &= 6.025738\text{PLR} - 22.38675\text{PRL}^2 + 31.6677\text{PLR}^3 \\ &\quad - 14.3232\text{PLR}^4 \end{aligned} \quad (1-3)$$

$$\text{EIRFLPM}(\text{dimensionless}) = 1.02503 - 0.000056778\text{CMH} \quad (1-4)$$

$$\text{EIRFRC}(\text{dimensionless}) = -5.3521 + 0.24069\text{RC} - 0.00197\text{RC}^2 \quad (1-5)$$

Table 1

Previous studies about VRF system.

Reference(s)	Author(s)	Outcomes
[3]	Yun, Y.Y.; Lee, J.H.; Kim, H.J.;	A load responsive control of the evaporating control in the VRF system, which aims to reduce the cooling energy consumption of the VRF system, has been developed Increasing the evaporating temperature can reduce the electricity consumption of the VRF system without impairing the energy efficiency of the VRF system. This simulation results demonstrate that the annual cooling energy consumption is lowered
[4]	Zang, R. et al.	The model categorizes the operations of the VRF-HR system into six modes based on the indoor cooling/heating requirements and the outdoor unit operational states, and develops particular algorithms for each mode to address various control logics The model has been adopted in the official release of the EnergyPlus simulation program since Version 8.6
[5]	Li, Y.M.; Wu, J.Y.:	In order to evaluate the energy features of the VRF system, a new energy simulation module is developed and embedded in the dynamic energy simulation program, EnergyPlus. And the indoor thermal comfort of the building in winter and the setting temperature of the system are analyzed If the HR-VRF system adopts the same temperature control method as the heat pump VRF (HP-VRF) system, the HR-VRF system promises 15–17% energy-saving potential, when compared to the HP-VRF system
[6]	Kim, D.S. et al.	A comparison study between the simulation results of VRF and RTU-VAV models is made to demonstrate energy savings potential of VRF systems The simulation results show that the VRF systems would save around 15–42% and 18–33% for HVAC site and source energy uses compared to the RTU-VAV systems
[7]	Aynur, T.N. et al.	The secondary components (indoor and ventilation units) of the VRF AC system promised 38.0–83.4% energy-saving potential depending on the system configuration, indoor and outdoor conditions, when compared to the secondary components (heaters and the supply fan) of the VAV AC system Overall, it was found that the VRF AC system promised 27.1–57.9% energy-saving potentials depending on the system configuration, indoor and outdoor conditions, when compared to the VAV AC system
[8]	Lee, J.H.; Im, P.; Song, Y.H.;	This Study was carried out field test and simulation evaluation of variable refrigerant flow systems performance The field test result showed that when energy consumptions of two systems were compared at the same outdoor conditions using the weather-normalized model, the VRF system exhibited energy reduction during cooling operation using simulations showed that the VRF system reduced more energy consumption

$$BGR \text{ (kWh)} = OUER/0.99 \tag{2}$$

$$P_{CT}(\text{kW}) = -0.0000000001\text{gwlp}m^3 + 0.0000008\text{gwlp}m^2 - 0.0017\text{gwlp}m + 5.5587 \tag{3}$$

$$FF(\text{kg/s}) = m/m_{\text{design}} \tag{4}$$

$$f_{pl}(\text{dimensionless}) = 0.0023 + 0.684FF - 1.8832FF^2 + 2.2FF^3 \tag{4-1}$$

$$Q_{\text{tot}}(\text{W}) = f_{pl}m_{\text{design}}\Delta P/(e_{\text{tot}}\rho_{\text{air}}) \tag{4-2}$$

From the factor analysis using these equations, the supply air temperature from the AHU, the flow rate and temperature of the warm condensing fluid, and the refrigerant condensing temperature were found to be the important determinants for calculating the energy consumption of the heating system. These values were selected as the input variables for the ANN model.

### 2.2. Artificial neural network and applications

The ANN, which is an engineering analogy of the human neural

**Table 2**  
Previous studies using the ANN for building thermal controls.

Reference(s)	Author(s)	Outcomes
[17,18]	Yeo, M.S.; Kim, K.W.; Yang, I.H.;	Two ANN models were developed for calculating the ascending and descending times of the current indoor temperature to the designated setpoint temperatures The calculated times were used to determine the optimal start and stop moments of the heating system at the opening and closing periods of the office building
[19]	Moon, J.W.; Jung, S.K.	Two ANN models and two control algorithms were proposed to suggest the energy-efficient setback value and period for an unoccupied period These proposed algorithms showed better performance in terms of energy efficiency and thermal comfort than the conventional algorithm
[20]	Ben-Nakhi, A.E.; Mahmoud, M.A.	An ANN model was developed to predict the optimal end of the setback moment (i.e., beginning of the normal period) of the cooling system in the commercial buildings The model predicted successfully, with strong correlation between the prediction results and the simulated results
[21]	Morel, N. et al.	Three ANN models were developed to predict future indoor temperature, outdoor temperature, and solar radiation, respectively A domestic radiant heating system provided more comfortable thermal condition with improved energy-efficiency using these predicted values
[22,23]	Lee, J.Y. et al.	An ANN model was proposed for operating a radiant under-floor heating system The overshoots and undershoots of the indoor temperature out of the comfortable range were significantly reduced
[24–26]	Moon, J.W.	Three ANN models were developed for conditioning the indoor air temperature, humidity, and PMV of domestic buildings ANN-based methods controlled the heating, cooling, humidifying, and dehumidifying systems, and provided a more comfortable and stable thermal environment
[27,28]	Argiriou, A.A. et al.	An ANN model was developed for the optimal control of the hydronic heating systems in solar buildings The proposed ANN-based method significantly reduced energy consumption for heating
[29]	Abbassi, A.; Bahar, L.	An ANN model was proposed to control an evaporative condenser The ANN-based method reduced process errors compared to the existing PID controller
[30]	Li, N. et al.	ANN-based control strategy for a direct expansion air conditioning system was developed, which simultaneously considered indoor air temperature and humidity The ANN-base controller was able to control the indoor air temperature and humidity by changing the compressor speed and supply fan speed
[31–33]	Hikmet, E. et al.	ANN-based prediction models were developed for operating a ground-coupled heat pump system They provided accurate calculation results for the coefficient of performance of the ground-coupled heat pump system
[34]	Chow, T.T. et al.	ANN and Genetic algorithm (GA) was proposed in an incorporative manner for the optimal use of electricity and fuel by an absorption chiller system The ANN model accurately calculated the coefficient of performance of the system, the mass flow rated of diesel oil, and electric power of the cooling water pump and chilled water pump
[35]	Ferreira, P.M. et al.	A predictive methodology was suggested for achieving energy saving and constant thermal comfort from an existing HVAC system control experiment The amount of energy saving reached over 50%
[36–40]	Moon, J.W. et al.	ANN-based models and algorithms were developed for the optimal control of a double skin façade depending on the external climate, indoor air temperature, indoor occupancy rate, and opening conditions The ANN model could respond to any external and internal environment changes, and maintain indoor thermal comfort to control the heating or cooling systems
[41]	Song, Z. et al.	A velocity propagation method was proposed based on a dynamic compact zonal model for a data center, and the results from a VPM zonal model and computational fluid dynamics (CFD) simulation were compared The results showed that the air flow and temperature distributions were in good agreement with those obtained using the zonal method and the CFD simulation results, which provided effective thermal control with limited monitoring of zonal temperature and air flow
[42]	Castilla, M. et al.	The ANN-based model for approximating thermal comfort evaluation was suggested for economic benefits by reducing the network sensor size for the real-time control of HVAC systems

system and learning process, is an empirical model that learns from experience and generalized data for prediction, pattern recognition, function approximation, optimization, and association [15]. One of the most popular and widely applied models is the multilayer feedforward network [16]. The fundamental structure of the network is composed of an input layer, hidden layer(s), and an output layer. Each layer can contain a series of nodes according to the model requirements. Each node in one layer is connected to every node in the next layer. Nodes are connected to each other with specific weights. The outgoing values of each node are weighted to have a different effect on the next node. The weighted incoming values to the next node are summed and transferred as an output of the current node. The identical process is repeated until the nodes in the output layer produce the output.

ANNs have been increasingly applied to building environmental controls. Various research efforts have dealt with ANN-based predictive approaches to control thermal control systems, including heating, ventilation, and air-conditioning (HVAC) systems, to improve indoor TC and to reduce energy consumption. Table 2 summarizes recent relevant studies. From these studies, the ANN-based thermal control methods present the potential for providing a comfortable thermal environment with advanced energy efficiency. These advantages provide the fundamental basis for developing ANN-based the VRF system control algorithm in this study.

### 3. Development process of the predictive model and control algorithm

Two major processes were conducted for proposing the energy-effective predictive heating system control method. The first process was to develop a predictive ANN model. The ANN model was developed for predicting the energy cost during the next control cycle and its prediction performance was tested using the measured data in the actual building in the preceding research [3]. The second process was to develop a control algorithm in which the ANN model was embedded. Using the predicted results from the ANN model, the algorithm determined the most cost-effective operating setpoints for the heating system. In this study, the performance tests for the developed ANN model and the control algorithm were conducted using computer simulation for the prediction accuracy and energy efficiency in terms of cost and consumed energy.

#### 3.1. ANN model for predicting energy cost

In the preliminary study conducted by Park et al. [9], an ANN model was developed to calculate the energy cost for the heating system during the next control cycle, which in this study was assigned as 5 min. Fig. 2 shows the structure of the ANN model. The model is composed of three layers—an input layer, a hidden layer, and an output layer. The input layer is composed of ten input neurons, which are relevant variables to determine the heating energy cost. They are: (1) the average outdoor air temperature for the last control cycle ( $t_{OA}$ ); (2) the average indoor air temperature of zones for the last control cycle ( $t_{IA}$ ); (3) the average supply air temperature of AHUs for the last control cycle ( $t_{SA}$ ); (4) the average condenser fluid temperature for the last control cycle ( $t_{CF}$ ); (5) the average condensing warm fluid amount for the control cycle ( $V_{CF}$ ); (6) the average heating load for the last control cycle ( $LOAD_{HEAT}$ ); (7) the setpoint of the AHU supply air temperature ( $t_{SA\_SET}$ ); (8) the setpoint of the condenser fluid temperature ( $t_{CF\_SET}$ ); (9) the setpoint of the condenser fluid amount ( $V_{CF\_SET}$ ); and (10) the setpoint of the refrigerant condensing temperature ( $t_{RF\_SET}$ ). Table 3 summarizes the ranges of input variables, and the values were normalized between 0 and 1 when they were applied to the ANN model.

Among these input variables, the first six variables are the results during the last control cycle, which are measured, and cannot be changed. On the other hand, the last four variables are the setpoints of the heating system for the next control cycle. These setpoints are not

determined at the beginning moment of the control cycle, which will be optimally determined in the control algorithm. The output of the ANN model is used as a determinant in the control algorithm.

The number of hidden layers and hidden neurons are 1 and 15, respectively. These numbers were determined as optimal in the preliminary research [9], which produced the most accurate prediction results. In that study, ANN models of 1–5 hidden layers with 15–25 hidden neurons were compared for their prediction performance. The ANN model with 1 hidden layer and 15 hidden neurons showed the most accurate prediction results.

In addition, the output of the ANN model is the total energy cost for heating ( $COST_{TOT}$ ), which is the sum of gas cost and electricity cost. The gas and electricity costs were assumed to be 689 Korean won/ $m^3$  (approximately 0.62 US\$/ $m^3$ ) and 143 Korean won/kWh (approximately 0.13 US\$/kWh), respectively, for the year 2017.

A sigmoid function and a pure linear function were used as transfer functions for hidden neurons and the output neuron, respectively. The initial learning rate (LR) and momentum (MO) were 0.5 and 0.4, respectively, which were found as optimal values in the preliminary study [9]. A total of 1000 training data sets were applied to train the ANN model. In addition, the sliding-window method was used for the data management of the training data sets; thus, when a new set was acquired, the oldest set was removed.

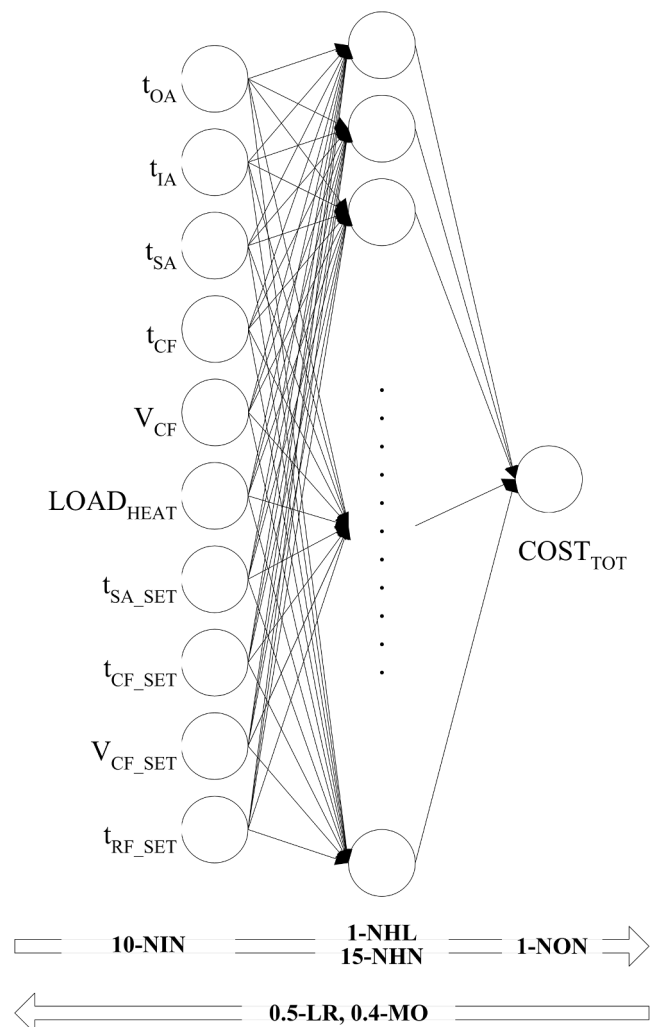


Fig. 2. Structure of the ANN model.

**Table 3**  
Normalized range by input variables.

Input	Normalized range
$t_{OA}$	–20 to 20 °C
$t_{IA}$	15–30 °C
$t_{SA}$	34–40 °C
$t_{CF}$	15–25 °C
$V_{CF}$	800–1800 L/min
$LOAD_{HEAT}$	0–300 kWh
$t_{SA\_SET}$	34–40 °C
$t_{CF\_SET}$	15–25 °C
$V_{CF\_SET}$	800–1800 L/min
$t_{RF\_SET}$	37–46 °C

**3.2. Model predictive control algorithm**

The ANN model was embedded in the control algorithm, which was developed using MATLAB (MathWorks, Natick, MA, US) software and its neural network toolbox. Fig. 3 shows the flow of the algorithm. The control algorithm starts its function by collecting the outdoor and indoor thermal conditions, followed by collecting the heating system operation conditions during the previous control cycle, which will be used in the ANN model.

If the current indoor temperature ( $t_{CUR\_IA}$ ) is lower than the indoor setpoint temperature ( $t_{SETPOINT}$ ), the embedded ANN model predicts the energy cost ( $COST_{TOT}$ ) for the next control cycle for the combinations of the four setpoints of the heating system— $t_{SA\_SET}$ ,  $t_{CF\_SET}$ ,  $V_{CF\_SET}$ , and  $t_{RF\_SET}$ . The energy costs for the different setpoint combinations are compared, and the optimal combination is found. The heating system will then work following the optimal setpoints. Fig. 4 conceptually presents the relevant part in the control algorithm that predicts, compares, and finds the optimal setpoint combination. The step size in Fig. 4 for assigning values to each variable was 1 °C, 1 °C, 100 L/min, and 1 °C for  $TEMP_{SA\_SET}$ ,  $TEMP_{CF\_SET}$ ,  $AMOUNT_{CF\_SET}$ , and  $TEMP_{RF\_SET}$ , respectively.

**4. Performance tests**

The performance of the predictive control algorithm embedding the ANN model was tested in comparison with the conventional algorithm. The performance evaluation was conducted to validate the prediction accuracy, results of the setpoint determination, and the amount and cost of the heating energy consumption. Table 4 summarizes the setpoints of the control variables for the conventional and predictive algorithms. The conventional algorithm used the fixed setpoints for the control variables of the heating systems, which is the strategy that is normally applied in the field. Meanwhile, the predictive algorithm considered a certain range for each control variable, and determined the most cost-effective combination using the prediction results from the ANN model. Thus, the values would be varied based on the determination by the predictive control algorithm.

The test building for the performance tests was an R&D center located in Seoul, South Korea (37.33°N latitude and 126.58°E longitude). It is an 11-story office building (Fig. 5) constructed in 2015 that covers a gross floor area of 22,660 m<sup>2</sup>. Offices, meeting rooms, and a lobby comprise the standard floor from the first to the tenth level. The monitoring variables are summarized in Table 5.

The building is equipped with a DX AHU water source VRF system. The test building was divided into 33 thermal zones using 11 AHUs and 37 outdoor units. Two to four outdoor units were connected to one AHU. AHUs and their covering zones are summarized in Table 6.

The performance tests were conducted using computer simulation. Three software programs—EnergyPlus (U.S. DOE) [44], MATLAB [45], and Building Controls Virtual Test Bed (BCVTB, U.S. DOE) [46] were applied in an incorporative manner for modeling the building and the

VRF system. Fig. 6 shows an overall diagram of the model including the data exchange. EnergyPlus software was used to model the VRF heating control system and produce the indoor thermal conditions. MATLAB software supplied the neural network (NN) toolbox, which was used to develop the ANN predictive model and control algorithm. The model and algorithm received the values for input neurons from EnergyPlus, and sent the system operating setpoints, such as  $t_{SA\_SET}$ ,  $t_{CF\_SET}$ ,  $V_{CF\_SET}$ , and  $t_{RF\_SET}$ , to the VRF system in EnergyPlus. In addition, additional functions were written for data management and storage. The BCVTB was a middleware, which connected the AHUs and outdoor units in EnergyPlus and the boiler, pumps, and control algorithm with the predictive model in MATLAB. Through this connection, the data produced in both software programs, EnergyPlus and MATLAB, could be transferred repeatedly.

The AHU discharge temperature setpoint was one of the main control variables, and thus the AHU discharge temperature should be maintained at the setpoint in each time-step, and the air flowrate should be modulated to meet the heating load. However, the water source VRF model in EnergyPlus was not able to maintain the AHU discharge temperature at the setpoint, and thus a work-around was implemented. Instead of using the water source VRF model, the air source VRF model (Coil:Heating:DX) in EnergyPlus was used in the system level; the plant level equipment, such as the boiler and pumps, were modeled in MATLAB. Even though the air source VRF model was applied, heat for evaporating refrigerant in the outdoor units was designed to be supplied using the heated water from the boiler instead of

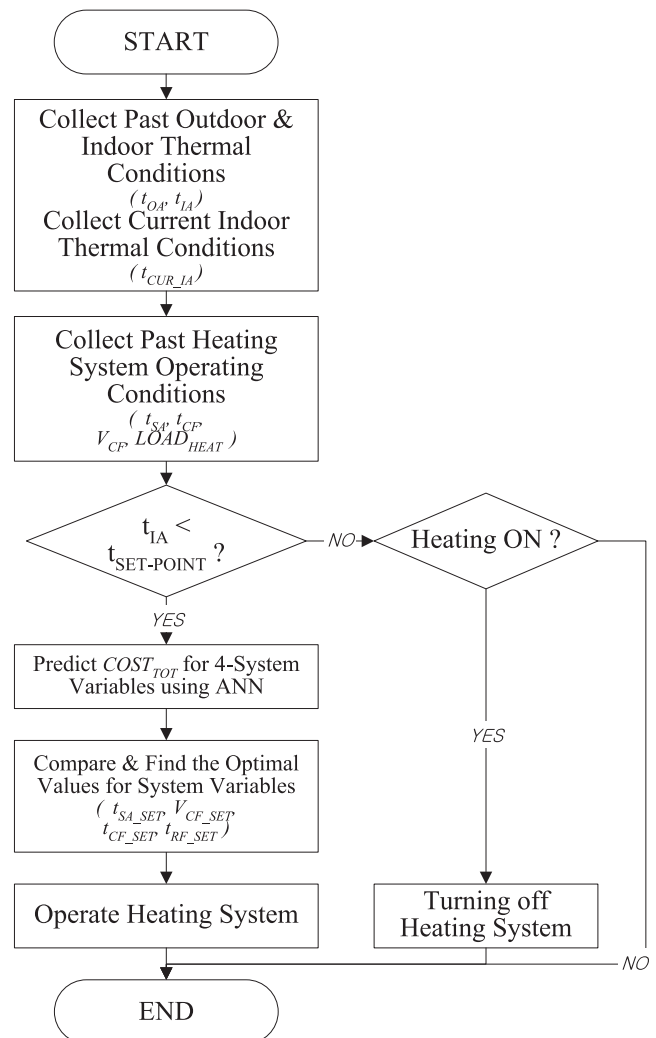


**Fig. 3.** Flowchart of the control algorithm.

For  $TEMP_{SA\_SET}$ , assign values from minimum to maximum by a specific step size  
 For  $TEMP_{CF\_SET}$ , assign values from minimum to maximum by a specific step size  
 For  $AMOUNT_{CF\_SET}$ , assign values from minimum to maximum by a specific step size  
 For  $TEMP_{RF\_SET}$ , assign values from minimum to maximum by a specific step size

*Predict the  $COST_{TOT}$  using ANN model*  
*Compare  $COST_{TOT}$  for the different set-point combination*  
*Find the set-point combination consuming the least  $COST_{TOT}$*

end  
 end  
 end  
 end

Fig. 4. Scheme to find the optimal setpoint combination.

Table 4  
 Setpoints of the control variables.

Control variables	Control algorithms	
	Conventional	Predictive
$t_{SA\_SET}$	38 °C	34–40 °C
$t_{CF\_SET}$	20 °C	15–25 °C
$V_{CF\_SET}$	1666 L/min	800–1800 L/min
$t_{RF\_SET}$	43 °C	37–46 °C

Table 5  
 Monitored variables and measuring time.

Variables	The unit of measuring time
Indoor dry-bulb temperature	5 min
Outdoor dry-bulb temperature	5 min
Outdoor relative humidity	5 min
Supply air dry-bulb temperature	5 min
Condenser fluid supply temperature of boiler	5 min
Condenser fluid volume flow rates	5 min
Energy used cost by the outdoor units	1 h
Energy used cost by the boiler	1 h
Energy used cost by the pumps	1 h
Energy used cost by the fans in the AHU	1 h

Table 6  
 AHU and zone composition.

VRF AHU number	Zones
1	1F_Lobby
2	1F_Conference Room, 2F_Conference Room
3	2F_Lobby
4	3F_ZoneA, 4F_ZoneA, 5F_ZoneA, 6F_ZoneA
5	3F_ZoneB, 4F_ZoneB, 5F_ZoneB, 6F_ZoneB
6	3F_ZoneC, 4F_ZoneC, 5F_ZoneC, 6F_ZoneC
7	3F_ZoneD, 4F_ZoneD, 5F_ZoneD, 6F_ZoneD
8	7F_ZoneA, 7F_ZoneC, 8F_ZoneA, 8F_ZoneC, 9F_ZoneA, 9F_ZoneC
9	7F_ZoneB, 8F_ZoneB, 9F_ZoneB
10	7F_ZoneD, 8F_ZoneD, 9F_ZoneD
11	10F_ZoneA

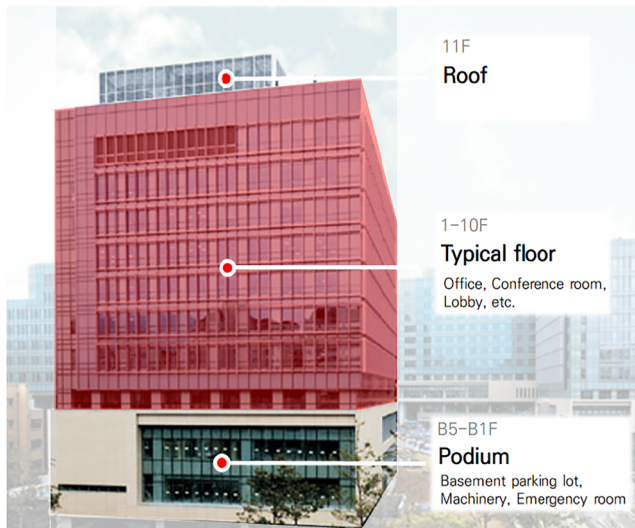


Fig. 5. The test building front view [43].

using the outdoor air. Therefore, the E+ model could realize the functions of the water source VRF system. The data exchange necessary to link the EnergyPlus–MATLAB model, such as the warm fluid temperature and flowrate, outdoor unit load, and energy consumption, was achieved through the BCVTB, which is the middleware software allowing users to couple different simulation programs for co-simulation.

The EnergyPlus–MATLAB model was validated and calibrated against the three-month measured data in the actual R&D center. In particular, the outdoor unit performance modeling requires three performance curves: (1) the capacity modifier, as functions of the DX coil

inlet air temperature, entering fluid temperature, and flowrate; (2) the energy input modifier, as functions of the DX coil inlet air temperature, entering fluid temperature, and flowrate; and (3) the energy input modifier, as a function of the part load ratio.

After the calibration process, the coefficient of variation root mean square error (CVRMSE) of the outdoor unit energy consumption between simulated and measured data was 15.2% [47], as shown in Fig. 7, indicating that the model is reliable enough to be used for this study, because it was less than the acceptable value of 30.0% that is suggested by ASHRAE (the American Society of Heating, Refrigerating and Air-Conditioning Engineers) Guideline 14: Measurement of energy and demand savings [48]. Thus, the validity of the simulation model is verified.

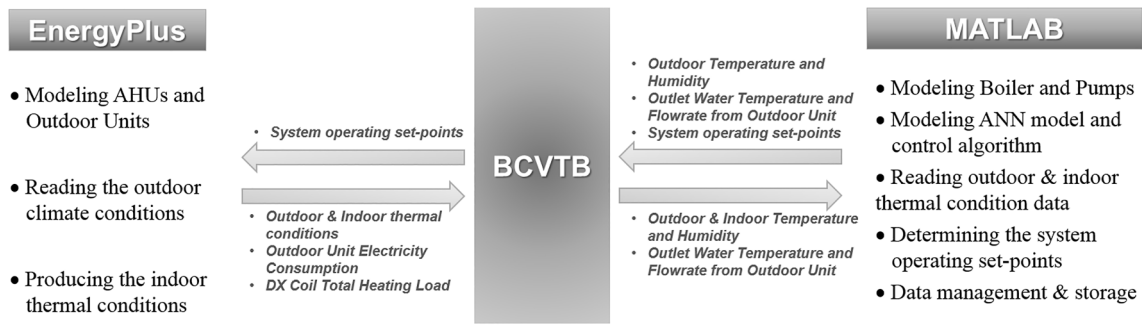


Fig. 6. The simulation method using the three software programs.

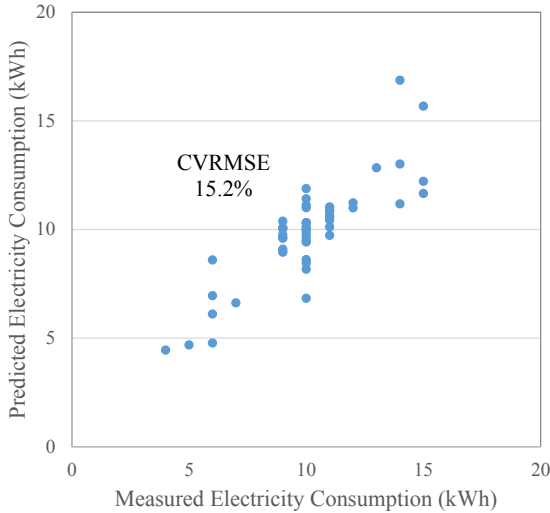


Fig. 7. CVRMSE between the predicted and simulated results.

5. Results analysis

The performance evaluation was conducted in terms of three categories—prediction accuracy of the ANN model, results of the setpoint determination, and amount and cost of the heating energy. The energy amount and cost was calculated for the case where the indoor temperature followed well to the designated setpoint temperature (21 °C). The indoor temperature was stabilized at 21 °C following the indoor setpoint temperature because the amount of heat supply to the indoor space is adjusted by the supply air temperature and amount for satisfying the setpoint temperature.

Fig. 8 shows the difference between simulated energy cost and the predicted energy cost. In most cycles, heating was not required in the test building. The number of cycles when the heating system worked was 1283 times, which means 6415 min. This is 7.55% of the total test period, which was 58 days in winter, from January 1st to February 28th. The average energy cost for each control cycle was 5317.6 Korean won (US\$ 4.78) and 5043.2 Korean won (US\$ 4.54) for the simulation and prediction, respectively. The difference between the simulated and predicted energy cost was higher at the earlier test period, then reduced after a certain period. The maximum difference was 1680 Korean won (US\$ 1.53) and the average difference was 274.4 Korean won (US\$ 0.25) for the 5-min control cycle. The CVRMSE between the simulated and predicted results was 7.42%. This number is under 30%, which is regarded as an acceptable value by ASHRAE Guideline 14: Measurement of energy and demand savings [48]. Thus, the prediction accuracy of the ANN model in this study is verified.

Fig. 9 shows how the control algorithm, which embedded the ANN model and used the prediction results, determined the optimal setpoints for the heating system operation. For most of the period that required

the heating operation, the  $t_{SA\_SET}$ ,  $t_{CF\_SET}$ ,  $V_{CF\_SET}$ , and  $t_{RF\_SET}$  were stably set to 38 °C, 25 °C, 1600 L/min, and 40 °C, respectively, except the early test period, during which the ANN model tuned itself to the simulation model. The most cost-efficient  $t_{SA\_SET}$  was the same as that of the conventional algorithm. On the other hand, the other three variables presented different setpoints to the conventionally assigned values (as previously given in Table 3). Although the optimal values are constant in this application, the values from the algorithm will vary in diverse applications with different backgrounds (e.g., different gas or electricity costs as well as different system or building capacities), which is due to the iterative self-training process of the ANN model. Following the variable setpoint values for the new environment, the building could be controlled in the most cost-efficient manner.

Fig. 10 shows the amount of energy consumption by the conventional and predictive algorithms. When the predictive algorithm was applied, the amount of gas consumption was increased. The amount of gas was 1666 m<sup>3</sup> and 2163 m<sup>3</sup> by the conventional and predictive algorithms, respectively. The electricity was reduced by the predictive algorithm. The amount of electricity was 41,120 kWh and 34,819 kWh by the conventional and predictive algorithms, respectively.

Fig. 11 shows the total energy cost by the conventional and predictive algorithms. The predictive algorithm saved significant energy cost caused by the optimal setpoints. This is because the predictive algorithm found the most cost-efficient setpoint combination for the control variables. Compared with the conventional method, which employed fixed values 38 °C, 20 °C, 1666 L/min, and 43 °C for  $t_{SA\_SET}$ ,  $t_{CF\_SET}$ ,  $V_{CF\_SET}$ , and  $t_{RF\_SET}$ , respectively, the cost savings by the predictive algorithm reached 7.93%, which was from 7,027,777 Korean won (US\$ 6,317.30) to 6,470,389 Korean won (US \$ 5,816.20). The amount of savings was 557,388 Korean won (US\$ 501.00). The significant savings was through the reduction of electricity consumption, which was 15.33% (901,080 Korean won, US\$ 810.00) from 5,880,224 Korean won (US\$ 5,825.70) to 4,979,144 Korean won (US \$ 4,475.80). On the other hand, the gas cost was slightly increased by 343,692 Korean won (US\$ 308.90).

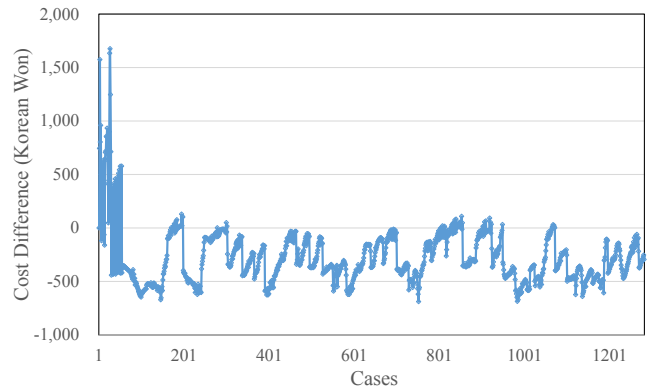


Fig. 8. Difference between the predicted cost and the simulated cost (simulated - predicted).

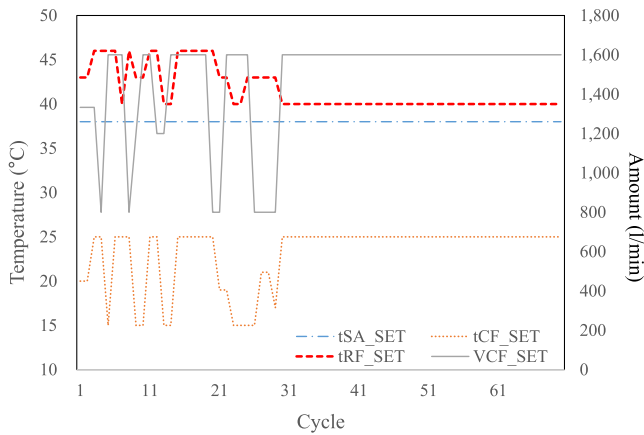


Fig. 9. Setpoints of variables determined by the predictive control algorithm.

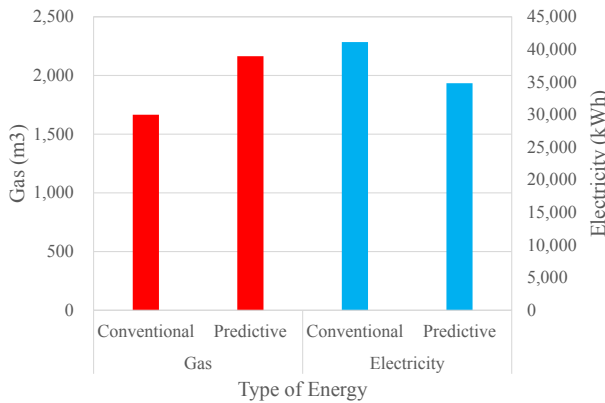


Fig. 10. The heating energy amount by the conventional and predictive algorithms.

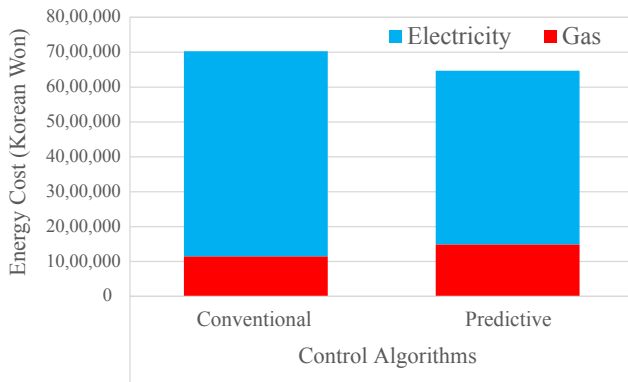


Fig. 11. The heating energy cost by the conventional and predictive algorithms.

The savings effect can be differentiated when the cost of gas and electricity is changed. If the gas cost rises to 1807 Korean won/m<sup>3</sup> (approximately 1.62 US\$/m<sup>3</sup>) from 689 Korean won/m<sup>3</sup> (approximately 0.62 US\$/m<sup>3</sup>), which was assumed in this study, no cost savings effect occurs. This means that the cost savings ratio decreases by as much as 0.79% per 10 cents increase of gas cost. However, using the iterative self-training process, the ANN model will reflect the changed energy cost and predict differently the energy cost for system operation. Thus, the result from the algorithm will propose different combinations of the variable setpoint values, which is the optimal solution in terms of cost.

Fig. 12 shows the energy cost for each component of the heating system. The electricity cost was related to the outdoor units, fans, and

pumps, while the gas cost was determined only by the boilers. The most significant component determining the energy cost was the outdoor units, which consumed approximately 73.3% and 65.7% of the total cost for the conventional and predictive algorithm, respectively. The savings percentage for the outdoor unit was 17.53% by the predictive algorithm. Since the outdoor units only use electricity, this savings directly impacted the electricity and cost savings.

On the other hand, as also explained in Figs. 10 and 11, the predictive algorithm increased the gas cost for the boiler. The cost was 1,147,553 Korean won (US\$ 1031.50) and 1,491,245 Korean won (US\$ 1340.50) for the two algorithms. The cost increase in the boiler is related to the decrease of electricity consumption in the outdoor unit. The algorithm was designed to find the most cost-effective setpoints. As shown in Fig. 12, the most significant energy-consuming component was the outdoor units. Thus, the predictive algorithm determined to operate the heating system in the manner of reducing the electricity consumption in the outdoor unit to save the total energy cost. In addition, the condenser heating rate through the refrigerant condensation was determined by adding the sum of the outdoor unit evaporator heat transfer rate for the refrigerant evaporation to the sum of outdoor unit electricity consumption. As mentioned earlier, the algorithm determined to reduce the electricity consumption in the outdoor units. Therefore, to maintain the same condenser heating rate through the refrigerant condensation between the conventional and optimized cases, the amount of heat supply from the boiler, which is the same as the sum of the outdoor unit evaporator heat transfer rate, should have been increased, resulting in the increase of gas consumption in the boiler.

## 6. Conclusions

In this study, a predictive algorithm was developed to cost-effectively operate an intermittently working VRF heating system. The algorithm determined the optimal setpoints for the heating system using an ANN model, which was designed to calculate the heating energy cost for the next control cycle. Using computer simulation, the performance of the predictive model and algorithm was tested in terms of the prediction accuracy of the ANN model, results of the setpoint determination, and amount and cost of the heating energy. A summary of our findings is as follows.

- (1) The prediction accuracy of the ANN model was proved by the low CVRMSE value between the simulated and predicted results. The CVRMSE was 7.42%, which is under the 30% level suggested as an acceptable value by the ASHRAE Guideline. Thus, the ANN model proved its potential to be applied in the control algorithm.

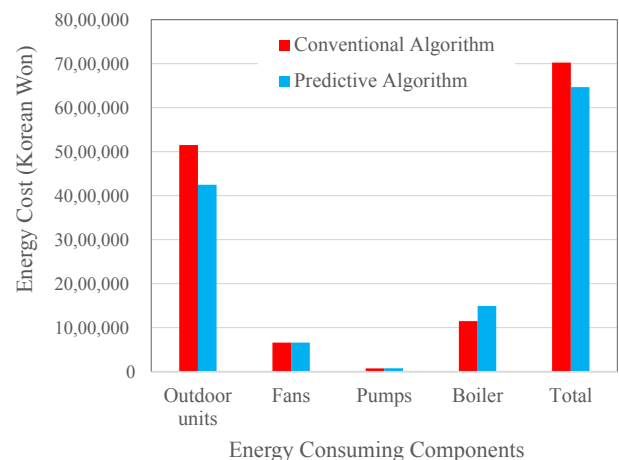


Fig. 12. Energy cost for each heating system component.

- (2) The predictive control algorithm stably determined the optimal setpoints for the heating system. For most periods,  $t_{SA\_SET}$ ,  $t_{CF\_SET}$ ,  $V_{CF\_SET}$ , and  $t_{RF\_SET}$  were stably set to 38 °C, 25 °C, 1600 L/min, and 40 °C, respectively.
- (3) The predictive control algorithm significantly saved on the heating energy cost. The total cost savings reached 7.93%. In particular, the significant savings was through the reduction of the electricity consumption in the outdoor units, which was 15.33%.
- (4) On the other hand, the gas cost was increased in the boiler. The gas cost increase was to increase the amount of heat supply to the condenser fluid in the boiler in order to maintain the amount of heat supply through the refrigerant condensation. The increased amount was 497 m<sup>3</sup>, which was from 1666 m<sup>3</sup> by the conventional algorithm, to 2163 m<sup>3</sup> by the predictive algorithm.

From the results analysis, the ANN model and the control algorithm presented the prediction accuracy and potential to control the intermittently working VRF heating system in a cost-effective manner. Further study is needed to test the control algorithm in actual buildings. In addition, an integrated control algorithm for the cooling system, as well as the heating system, needs to be developed to provide a more comfortable and cost-effective thermal environment.

### Acknowledgements

This research was supported by a grant (code 18CTAP-C129762-02) from Infrastructure and Transportation Technology Promotion Research Program funded by Ministry of Land, Infrastructure and Transport of Korean government and by a grant of the research fund of the MOTIE (Ministry of Trade, Industry and Energy, South Korea) in 2018. Project number: 20182010600010.

### Appendix A. Supplementary material

Supplementary data to this article can be found online at <https://doi.org/10.1016/j.applthermaleng.2018.12.044>.

### References

- [1] Y.K. Baik, J.W. Moon, Input variable decision of the predictive model for the optimal starting moment of the cooling system in accommodations, *Int. J. Korea Inst. Ecol. Archit. Environ.* 15 (2015) 105–110.
- [2] D. Zhang, X. Zhang, J. Liu, Experimental study of performance of digital variable multiple air conditioning system under part load conditions, *Energy Build.* 43 (2011) 1175–1178.
- [3] G.Y. Yun, J.H. Lee, H.J. Kim, Development and application of the load responsive control of the evaporating temperature in a VRF system for cooling energy savings, *Energy Build.* 116 (2016) 638–645.
- [4] R. Zang, K. Sun, T. Hong, Y. Yura, R. Hinokuma, A novel Variable Refrigerant Flow (VRF) heat recovery system model: development and validation, *Energy Build.* 168 (2018) 399–412.
- [5] Y.M. Li, J.Y. Wu, Energy simulation and analysis of the heat recovery variable refrigerant flow system in winter, *Energy Build.* 42 (2010) 1093–1099.
- [6] D. Kim, S.J. COX, H. Cho, P. Im, Evaluation of energy savings potential of variable refrigerant flow (VRF) from variable air volume (VAV) in the US climate locations, *Energy Rep.* 3 (2017) 85–93.
- [7] T.N. Aynur, Y. Hwang, R. Radermacher, Simulation comparison of VAV and VRF air conditioning systems in an existing building for the cooling season, *Energy Build.* 41 (2009) 1143–1150.
- [8] J.H. Lee, P. Im, Y.H. Song, Field test and simulation evaluation of variable refrigerant flow systems performance, *Energy Build.* 158 (2018) 1161–1169.
- [9] B.R. Park, E.J. Choi, J. Hong, J.H. Lee, J.W. Moon, Development of an energy cost prediction model for a VRF heating system, *Appl. Therm. Eng.* 140 (2018) 476–486.
- [10] The U.S. D.O.E., EnergyPlus Engineering Reference V. 8.5; The Reference to EnergyPlus Calculations, Chapter 15.11.1 Variable Refrigerant Flow Heat Pump Model (System Curve Based Model), 2011, p. 1121.
- [11] Samsung Electronics Co., DVM S Water Technical Data Book, 2015.
- [12] The U.S. D.O.E., EnergyPlus Engineering Reference V. 8.5; The Reference to EnergyPlus Calculations, Chapter 15.17.3 Variable Speed Pump, 2011, p. 1257.
- [13] The U.S. D.O.E., EnergyPlus Engineering Reference V. 8.5; The Reference to EnergyPlus Calculations, Chapter 15.9.2.3 Simulation, 2011, p. 1015.
- [14] The U.S. D.O.E., EnergyPlus Input Output Reference V. 8.5; The Reference to EnergyPlus Calculations, Chapter 1.41.3 Fan: Variable Volume, 2011, p. 1907.
- [15] I.D. Basheer, M. Hajmeer, *Artificial neural networks: fundamentals, computing, design, and application*, *J. Microbiol. Meth.* 43 (2000) 3–31.
- [16] G. Zhang, B.E. Patuwo, M.Y. Hu, Forecasting with artificial neural networks: the state of the art, *Int. J. Forecast.* 14 (1998) 35–62.
- [17] I.H. Yang, M.S. Yeo, K.W. Kim, Application of artificial neural network to predict the optimal start time for heating system in building, *Energy Convers. Manage.* 44 (2003) 2791–2799.
- [18] I.H. Yang, K.W. Kim, Development of artificial neural network model for the prediction of descending time of room air temperature, *Int. J. Air-Cond. Refrig.* 12 (2000) 1038–1048.
- [19] J.W. Moon, S.K. Jung, Development of a thermal control algorithm using artificial neural network models for improved thermal comfort and energy efficiency in accommodation buildings, *Appl. Therm. Eng.* 103 (2016) 1135–1144.
- [20] A.E. Ben-Nakhi, M.A. Mahmoud, Energy conservation in buildings through efficient A/C control using neural networks, *Appl. Energy* 73 (2002) 5–23.
- [21] N. Morel, M. Bauer, M. El-Khoury, J. Krauss, NEUROBAT, a predictive and adaptive heating control system using artificial neural networks, *Int. J. Sol. Energy* 21 (2001) 161–201.
- [22] J.Y. Lee, M.S. Yeo, K.W. Kim, Predictive control of the radiant floor heating system in apartment buildings, *J. Asian Archit. Build. Eng.* 1 (2002) 105–112.
- [23] J.Y. Lee, I.H. Yang, S.Y. Song, H.S. Kim, K.W. Kim, A study of the predictive control of the on/off system in apartments, *Proceedings of the International Building Performance Simulation Association*, 1999, pp. 215–222.
- [24] J.W. Moon, J.J. Kim, ANN-based thermal control methods for residential buildings, *Build. Environ.* 45 (2010) 1612–1625.
- [25] J.W. Moon, ANN-based Model-free Thermal Controls for Residential Building (Ph.D. Dissertation), Taubman College of Architecture and Urban Planning, University of Michigan, Ann Arbor, 2009.
- [26] J.W. Moon, Performance of ANN-based predictive and adaptive thermal control methods for disturbances in and around residential buildings, *Build. Environ.* 48 (2011) 15–26.
- [27] S.S. Argiriou, I. Bellas-Velidis, M. Kummert, P. Andre, A neural network controller for hydronic heating systems of solar buildings, *Neural. Netw.* 17 (2004) 424–440.
- [28] A.A. Argiriou, I. Bellas-Velidis, C.A. Balaras, Development of a neural network heating controller for solar buildings, *Neural. Netw.* 13 (2000) 811–820.
- [29] A. Abbassi, L. Bahar, Application of neural network for the modeling and control of evaporative condenser cooling load, *Appl. Therm. Eng.* 25 (2005) 3176–3186.
- [30] N. Li, L. Xia, D. Shiming, X. Xu, M.Y. Chan, Dynamic modeling and control of a direct expansion air conditioning system using artificial neural network, *Appl. Energy* 91 (2012) 290–300.
- [31] E. Hikmet, I. Mustafa, S. Abdulkadir, E. Mehmet, Forecasting of a ground-coupled heat pump performance using neural networks with statistical data weighting pre-processing, *Int. J. Therm. Sci.* 47 (2008) 431–441.
- [32] E. Hikmet, I. Mustafa, S. Abdulkadir, E. Mehmet, Artificial neural networks and adaptive neuro-fuzzy assessments for ground-coupled heat pump system, *Energy Build.* 40 (2008) 1074–1083.
- [33] E. Hikmet, I. Mustafa, S. Abdulkadir, E. Mehmet, Performance prediction of a ground-coupled heat pump system using artificial neural networks, *Expert Syst. Appl.* 35 (2008) 1940–1948.
- [34] T.T. Chow, Z. Lin, C.L. Song, G.Q. Zhang, Applying neural network and genetic algorithm in chiller system optimization, *Proceedings of the Seventh International Building Performance Simulation Association*, Rio de Janeiro, Brazil, 2001, pp. 1059–1065.
- [35] P.M. Ferreira, A.E. Ruano, S. Silva, E.Z.E. Conceição, Neural networks based predictive control for thermal comfort and energy savings in public buildings, *Energy Build.* 55 (2012) 238–251.
- [36] J.W. Moon, J.H. Lee, Y. Yoon, S. Kim, Determining optimum control of double skin envelope for indoor thermal environment based on artificial neural network, *Energy Build.* 69 (2014) 175–183.
- [37] J.W. Moon, J. Lee, J.D. Chang, S. Kim, Preliminary performance tests on artificial neural network models for opening strategies of double skin envelopes in winter, *Energy Build.* 75 (2014) 301–311.
- [38] J.W. Moon, Integrated control of the cooling system and surface openings using the artificial neural networks, *Appl. Therm. Eng.* 78 (2015) 150–161.
- [39] J.W. Moon, Comparative performance analysis of the artificial-intelligence-based thermal control algorithms for the double-skin building, *Appl. Therm. Eng.* 91 (2015) 334–344.
- [40] J.W. Moon, Development of integrated control methods for the heating device and surface openings based on the performance tests of the rule-based and artificial-neural-network-based control logics, *Korea Inst. Ecol. Archit. Environ.* 14 (2014) 97–103.
- [41] Z. Song, B.T. Murray, B. Sammakia, A dynamic compact thermal model for data center analysis and control using the zonal method and artificial neural networks, *Appl. Therm. Eng.* 62 (2014) 48–57.
- [42] M. Castilla, J.D. Álvarez, M.G. Ortega, M.R. Arahal, Neural network and polynomial approximated thermal comfort models for HVAC systems, *Build. Environ.* 59 (2013) 107–115.
- [43] I. Kang, H.L. Lee, J.H. Lee, J.W. Moon, Artificial neural network-based control of a variable refrigerant flow systems in the cooling season, *Energies* 11 (2018) 1–15.
- [44] EnergyPlus, EnergyPlus; 2018-10. Available from: < <https://energyplus.net/> > .
- [45] Mathworks, MATLAB 14, vol. 26; 2018-10, pp. 10–17. Available from: < <http://www.mathworks.com> > .
- [46] Simulation Research, Building Controls Virtual Test Bed; 2018-10. < <https://simulationresearch.lbl.gov/bcvtb> > .
- [47] Samsung Electronics Co., Development of a MPC-based operating tool for the VRF system, Technical Report, 2017.
- [48] American Society of Heating, Refrigerating, and Air-Conditioning Engineers, Inc. ASHRAE Guideline14-Measurement of energy and demand savings. ASHRAE, 2002.